

01,07

## Cold brittleness of metals as a structural multistage dislocation process

© V.M. Chernov<sup>1,2</sup>

<sup>1</sup> A.A. Bochvar High-Technology Research Institute of Inorganic Materials,  
Moscow, Russia

<sup>2</sup> National Research Nuclear University MEPhI,  
Moscow, Russia

E-mail: VMChernov@bochvar.ru

Received March 3, 2023

Revised March 3, 2023

Accepted March 2023, 2023

The cold brittleness of metals under conditions „before — during — after“ irradiation in nuclear and thermonuclear reactors is considered. The conditions and mechanisms of cold brittleness are determined depending on the type of their crystal lattices, structures, physical and mechanical properties and external influences (temperature, stress, reactor irradiation). The mechanisms of cold brittleness are dislocational and define cold brittleness as a structural multistage process. Stress relaxation at the front of a subcritical crack stops its growth (cold brittleness is not formed). The stacking fault energy of the metal determines the critical level of stress for the beginning of its relaxation by mechanical twinning at the crack front (external stress concentrator). In irradiated metals (cold-brittle „before“ irradiation), the temperature range of cold-brittleness expands. „During“ irradiation, cold brittleness is not formed.

**Keywords:** alloys, steels, low temperatures, reactor irradiation, crack nucleation, brittle fracture, stages, mechanisms.

DOI: 10.21883/PSS.2023.05.56038.28

### 1. Introduction

The problem of cold brittleness and fracture resistance of metals (alloys, steels) has been studied for a long time [1–16], but is still pending for low temperature application of metals (products), including structural materials for nuclear and nuclear fusion reactors. Cold brittleness and fracture resistance of metals (products) is determined by the occurrence of low temperature embrittlement (generation of ductile-brittle transition temperature  $T_{dbtt}$ ) in certain conditions (temperature, stress), initiation and propagation of subcritical and critical cracking and brittle failure at  $T < T_{dbtt}$  and external stresses lower than the metal yield strengths. To identify metal cold brittleness conditions, almost only Griffith model (1920 [1]) is available which defines critical fracture size  $L = \alpha(E\gamma/\sigma^2)$  as an energy criterion of cold brittleness occurrence in metals. Here,  $L$  is a fracture half-length,  $E$  is and elastic modulus of metal,  $\gamma$  is the specific surface energy of metal,  $\sigma$  is the normal stress to the crack plane. Coefficient value  $\alpha \approx 1$  is defined by the current geometry and metal (product) stress condition [1–16]. For further investigations of metal cold brittleness, Griffith condition includes only some corrections (adjustment of  $\alpha$ ) that take into account metal geometry, crack front shape, plastic zone and possible critical crack opening mechanisms [2–16].

Formation of cold brittleness condition (generation of  $T_{dbtt}$ ) and brittle failure of metals in such condition are defined by complex dislocation mechanisms defined by crystal lattices (BCC — body-centered cubic, FCC — face-centered cubic, HCP — hexagonal close-packed), structural

phase, temperature and stress conditions, slip systems, dislocation mobilities and physical and chemical properties (elasticity, strength) of metals. Cold brittleness is a typical property of BCC metals (exclusion — tantalum metal, Ta), does not occur in FCC metals and occurs in some HCP metals [6,10,16]. Some plastic strain of metals always precedes their brittle failure in cold brittleness condition [2]. cold brittleness occurs in mono- and polycrystalline metals. Modifications of structural phase conditions and low temperature strength of cold-brittle metals (alloying, impurities, thermomechanical treatment, irradiation) change the cold brittleness temperature threshold ( $T_{dbtt}$ ). At quasi-static mechanical loads (short-term mechanical test), temperature dependences of stress-strain properties (elasticity moduli, strength, ductility) of cold-brittle metals in their cold brittleness temperature regions have no special features [6,8,10,14–16].

Causes and physical mechanisms behind (non)occurrence of cold brittleness in metals depending on the type and properties of crystalline lattices (BCC, FCC, HCP) of composites, structural phase conditions and ambient conditions (temperature, reactor irradiation) are still insufficiently studied and solved. Such condition necessitates the investigation of cold brittleness of metals in conditions „before — during — after“ reactor irradiations. The outcome of such investigations is necessary for identification of cold brittleness temperature regions (measurement of  $T_{dbtt}$ ) and brittle failure mechanisms in the development of next generation structural materials (products) to meet the next generation equipment requirements, including nuclear and nuclear fusion reactors.

This study addresses and defines the following aspects as generalization and development of investigations of metal structure and stress-strain properties [14,15,17–26]:

- conditions and dislocation mechanisms of (non)occurrence of cold brittleness in metals depending on the types (BCC, FCC, HCP) and properties of their crystal lattices (types, slip systems and dislocation mobility and height of Peierls barriers), stress-strain properties (stacking fault and surface energies, elasticity, strength, ductility) and (stress, temperature) states in conditions „before — during — after“ reactor (neutron, gamma) irradiation.

- cold brittleness as gradual multistage structural dislocation process controlled by stress and temperature states of metals (products), initiation and propagation of subcritical and critical cracks (external stress risers) in them with stresses in the tips of cracks having various criticality level for properties of metals (dislocation initiation and mobility, mechanical twinning, shear, separation).

## 2. Cold brittleness of metal. Cold brittleness (brittle failure) stages

Further consideration of cold brittleness of metals (products) assumes that their initial states are free from cracks, metals (products) are exposed to low continuous uniform external stresses (lower than yield strengths) that form a certain stress state in metals (products). Difference in metal crystal lattice constants and Burgers dislocation vectors for different crystallographic directions is not considered. Difference in stress-strain states of samples (products) defined by their geometry and external load is not considered. Consideration of such features results in insufficient quantitative change of some numerical parameters (like coefficient  $\alpha$  in the foregoing Griffith condition).

External stress causes stress components  $\sigma_{ij}$  in the fracture plane ( $i, j = 1, 2, 3$ , coordinate system in the fracture propagation plane). Components  $\sigma_{12}$  and  $\sigma_{22}$  define shear and normal components of external stress in the fracture plane and their ratio  $\lambda = \sigma_{12}/\sigma_{22}$  defines the metal stress state severity.

### 2.1. Stage 1 (incubation). Crack initiation and growth

This stage takes place in all crystal classes of metals (BCC, FCC, HCP) and its length is defined by compositions, structural phase and fault states, dislocation slip systems and ambient conditions (stress, temperature). Plastic strain of metals at this stage is defined by slow thermally activated dislocation mobility that determines initiation (multipoint) and growth of subcritical cracks. Crack propagation direction (plane) depends on crystallography, stress state severity and structure (polycrystallinity, texture, etc.) of metal and may vary (side crack initiation) with slow crack propagation. Crack initiation (multipoint) and growth may occur both in a single crystalline plane and in adjacent parallel planes with formation of a crack initiation and propagation band (meso band).

### 2.2. Stage 2. Formation of critical cracks (cold-shortness pre-requisite)

Fracture is an external stress riser. For clarity, type I cracks (separation, elongation) will be addressed, because this type is of the most practical importance [6,10,16]. Stress occurs in the tip of the crack [16]:

$$\sigma_{ij}(r) = \sigma_{ij}[1 + (L/2r)^{1/2}] = \sigma_{ij} + K_{ij}/(2\pi r)^{1/2}, \quad (1)$$

where  $2L$  is the crack length,  $r$  is the radius (the origin of coordinates is in the tip of the crack),  $K_{ij} = \sigma_{ij}(\pi L)^{1/2}$  is the stress intensity coefficient in the tip of the crack representing the metal fracture resistance. Crack propagation direction (plane) is defined by stress component values  $\sigma_{ij}(r)$  in the tip and crystallography of the dislocation slip plane. Crack propagation plane direction may vary with slow crack growth (branching) depending on the crack propagation resistance (crystallography, faults, grain boundaries, texture, etc.) and metal (product) stress state severity.

Critical stress component values for mechanical twinning  $\sigma_{cr1} = \sigma_{sf}$ , shear  $\sigma_{cr2} = \sigma_{sh}$  and separation  $\sigma_{cr3} = \sigma_{br}$  of metal are typical stress component values in the crack tip (external stress riser) that define critical sizes and propagation rate of the crack. These critical stresses are defined by critical stresses of strain-induced stacking fault  $\sigma_{sf} = \sigma_{sf}/b \approx (0.05-0.1)G$  [5], shear  $\sigma_{sh} \approx 0.1G$  and separation  $\sigma_{br} = (E\gamma/a)^{1/2} \approx 0.3E$  of metal [4–11,16,27]. Here,  $G$  is the shear elastic modulus,  $E$  is the modulus of elasticity (Young's modulus),  $\gamma \approx 0.1Ea$  is the stacking fault energy,  $\gamma_{sf}$  is the stacking fault energy,  $a$  is the metal crystal lattice constant,  $b$  is the Burgers dislocation vector value.

Further crack propagation will vary depending on the sequence of achievement of critical stresses  $\sigma_{cr1}$ ,  $\sigma_{cr2}$  and  $\sigma_{cr3}$ . If mechanical twinning stress  $\sigma_{cr1} = \sigma_{sf}$  will be the first critical stress, then stress relaxation will occur in the subcritical crack tip (in case slow crack growth) and growth of such crack will stop (no critical crack is initiated, no cold brittleness is formed). Such crack formation condition may be implemented in metals with low stacking fault energies (FCC metals, some HCP metals, BCC Ta, see Section 5). If condition  $\sigma_{cr1} > \sigma_{cr3}$  is met, then critical crack is formed and its dynamic propagation will start in certain conditions. In case of quick dynamic propagation of a critical crack, stress relaxation in its tip is negligible.

Cold brittleness conditions for metals (subcritical crack formation and growth and dynamic propagation of critical cracks) will be met if there are no stress relaxation processes in the crack tips ( $\sigma_{cr1} > \sigma_{cr2}$ ,  $\sigma_{cr3}$ ).

When there is no stress relaxation in the tips of growing subcritical cracks, crack length achieves the critical shear crack size ( $\sigma_{ij} = \sigma_{sh}$ ):

$$L_{12sh} = 2a[\sigma_{sh}/\sigma_{12}]^2 \approx 0.02a(G/\sigma_{12})^2, \quad (2)$$

when only shear stress component (in crack plane)  $\sigma_{12}$  in the crack tip achieves critical metal shear stress  $\sigma_{12cr} = \sigma_{sh}$ .

Critical intensity of shear stress in the critical shear crack tip is defined by  $K_{I12cr} = (2\pi a)^{1/2}\sigma_{sh} \approx 0.25a^{1/2}G$  and characterizes shear fracture resistance (shear fracture) of metal at an appropriate temperature and geometry. Further propagation of the critical shear crack may occur by means of shear strain at the crack front in the crack plastic zone. During critical crack propagation, shear fracture of metal may occur depending on its geometry (cross-section area in the crack plane).

At the growing shear crack front, a plastic zone is formed where a shear stress component condition  $\sigma_{I12}(r) \geq \sigma_{ys}$  is met ( $\sigma_{ys}$  is the metal yield strength, constrained deformation). Size of this plastic zone  $R_{pl}$  for a crack with critical size  $L_{12sh}$  from (1) is defined by expression

$$R_{12pl} = (L_{12sh}/2)(\sigma_{12}/\sigma_{ys})^2 \approx a(\sigma_{sh}/\sigma_{ys})^2. \quad (3)$$

Dislocation initiation (dislocation placement) and mobility in the plastic zone of the critical shear fracture define the crack propagation rate. Effective size of the critical shear crack is defined by

$$L_{ef12sh} = L_{12sh} + R_{12pl} = L_{12sh} [1 + (1/2)(\sigma_{12}/\sigma_{ys})^2]. \quad (4)$$

With further growth (dislocation mechanisms), the critical shear crack achieves the critical separation crack length  $L_{22br}$ , when normal stress component  $\sigma_{122}$  in the crack tip achieves critical metal separation stress  $\sigma_{122} = \sigma_{122cr} = \sigma_{br}$ . The size of such critical (separation) stress is defined from (1) by

$$L_{22br} = 2a[\sigma_{br}/\sigma_{22}]^2 = 2E\gamma/(\sigma_{22})^2 \approx 0.2a(E/\sigma_{22})^2. \quad (5)$$

Critical crack size  $L_{22br}$  is defined by metal stress state (external stress component  $\sigma_{22}$  in the crack plane) and critical separation stress (elastic modulus, surface energy). Condition (5) is a pre-requisite for occurrence of cold brittleness in metal characterized by critical (separation) crack formation and is consistent with Griffith energy criterion ([1], above). Critical crack length  $L_{22br}$  and stress state (external stress component  $\sigma_{22}$ ) are interconnected by a relationship characterizing the cold brittleness (fracture resistance) of metal

$$(\sigma_{22})^2 L_{22br} = 2a(\sigma_{br})^2 = 2E\gamma \approx 0.2aE^2. \quad (6)$$

Stress intensity coefficient in the critical (separation) crack tip is defined by  $K_{I22cr} = (2\pi a)^{1/2}\sigma_b = (2\pi E\gamma)^{1/2} \approx 0.8a^{1/2}E$  and is a fracture resistance property of metal (product) at the appropriate temperature and geometry. Effective length of the critical (separation) crack, including its plastic zone ( $\sigma_{122}(r) > \sigma_{ys}$ , constrained deformation) will be defined by

$$\begin{aligned} L_{ef22br} &= L_{22br} [1 + (1/2)(\sigma_{22}/\sigma_{ys})^2] \\ &= L_{22br} + a(\sigma_{br}/\sigma_{ys})^2, \end{aligned} \quad (7)$$

where  $L_{22br}$  is defined by expression (5).

Simultaneous achievement of critical shear stress  $\sigma_{sh}$  and critical separation stress  $\sigma_{br}$  of metal in the critical crack tip defines a pre-requisite or cold brittleness (critical crack formation), if subsequent conditions of fast dynamic propagation of the formed critical crack are provided (next cold brittleness stage 3).

### 2.3. Stage 3. Fast dynamic propagation of the critical crack (sufficient dynamic cold brittleness condition)

This stage may occur in metals at their certain structural, strength, surface (surface energy), stress and temperature conditions that form cold brittleness temperature threshold ( $T_{dbtt}$ ). Critical crack propagation rate (external stress riser) is defined by dislocation mobility in its plastic zone (3). To form high dynamic dislocation slip velocity in the plastic zone of the crack, high shear (start) stress for dislocation initiation (Frank–Read source work) and dislocation movement (start), and low viscous dislocation drag („dry“ friction condition) are required.

Start stresses for dislocation initiation and slip in plastic zones of critical cracks are defined by potential pattern amplitudes (Peierls barriers, faults, phase particles) in dislocation slip planes. With temperature decrease, viscous dislocation drag level is reduced (phonon and electronic mechanisms) [4,5,28,29], and when critical temperature (physical temperature  $T_{dbtt}$ ) is achieved, viscous dislocation drag achieves its low (critical) value that defines occurrence of dynamic dislocation mobility region (with high start stress, „dry friction“ condition). High start stresses for dislocation mobility (slip) are defined by high potential energy pattern amplitudes in dislocation slip planes and primarily by high Peierls barriers.

In metal cold brittleness state, a local dynamically bound state „crack front — dislocation“ („frodic“) is formed in the critical crack propagation plane at the crack front. High start stress and high dynamic dislocation rate define high dynamic „frodic“ rate (critical crack propagation rate) increasing with the increase in crack size with asymptotic approach to the sound speed in metal [4,5,28,29].

Dynamic propagation conditions for the occurring critical (separation) crack are defined by metal (product) stress condition, stress at the crack front (external stress riser) and relationship of crack opening work (formation of two surfaces) and crack elongation work (dynamic dislocation slip). Critical crack propagation rate is defined by dynamic „frodic“ rate at the crack front (plastic zone) when dynamic condition is met [17,18]:

$$B(T)v(\sigma_{112}, T) < 2\gamma, \quad (8)$$

where  $B(T)$  is the viscous dislocation drag coefficient [4,5,28,29],  $T$  is the metal temperature,  $v(\sigma_{112}, T)$  is the dislocation rate in plastic zone of the propagating critical crack,  $\sigma_{112}$  is the shear stress in the crack tip in the crack plastic zone. Cold brittleness temperature threshold (physical temperature  $T_{dbtt}$ ) in metal defined by condition (8) depends on conditions in the plastic zone of the crack and metal properties that form dynamic „frodic“ mobility. Metal surface tension energy  $\gamma$  is defined by its crystal lattice (BCC, FCC, HCP), composition, crack plane crystallography and environment inside the crack. Surface energies of BCC metals are higher than surface energies of FCC metals [4,5], which also defines fulfilment of cold

brittleness occurrence condition in metals with different crystal lattices (implementation of criterium (8)). Dynamic dislocation mobility region in stronger (with higher fault content) metals moves towards a higher stress region (see Section 3). Dynamic dislocation rate („frodiss“ rate) increases with an increase in the crack size (increase in shear stress components in the dislocation slip plane), decreases with the increase in metal strength (increase in fault content), increases with temperature decrease and asymptotically approaches the sound speed in metal (see Section 3).

Dynamic condition (8) is sufficient for occurrence of cold brittleness in metals (without stress relaxation in subcritical crack tip) and supplements the cold brittleness pre-requisite (5).

#### 2.4. Stage 4. Critical area formation („open“ area) in the crack propagation plane

In the plane (meso band) of (multipoint) subcritical crack initiation and growth and of dynamic critical crack propagation, the area of retained and sophisticated („open“ area) cross section of metal (product) quickly decreases. When this cross-section area (meso band) decreases to the critical value defined by an increase in normal external stress component  $\sigma_{22}$  in this cross-section (at constant external load) up to the yield strength of metal  $\sigma_{ys}$  ( $\sigma_{22} \geq \sigma_{ys}$ ), plastic strain is initiated in the metal normally to the crack propagation plane (band). Effective area of such cross section includes corresponding plastic zones in the crack tips (3), and the size of this cross section is equal to a fraction ( $\sigma_{22}/\sigma_{ys}$ ) of the initial cross-section area and may be achieved (in case of multipoint crack initiation) earlier than a critical crack is formed. Formation time of such critical cross section in metal (product) cold brittleness conditions virtually defines metal performance time (lifetime) at these sizes and ambient conditions (temperature, stress conditions).

#### 2.5. Stage 5. Plastic strain-to-fracture of cold-brittle metals

After formation of critical cross-section area in metal (stage 4), regular strain-to-fracture starts in the metal under the influence of normal tensile stress  $\sigma_{22}$  ( $\sigma_{22} \geq \sigma_{ys}$ ) with formation of two separation surfaces. Separation surfaces will have complex (fractal) patterns (ingeneral, different) formed at different cold brittleness stages (stages 1–4) and by regular metal strain-to-failure (stage 5). Complex metal failure surface patterns are formed by its microstructure (crystallography, polycrystallinity, texture, phase particles), initiation (multipoint, including adjacent parallel planes) and propagation of subcritical and critical cracks (by shear, separation) up to formation of a critical metal (product) cross-section followed by regular low-temperature strain-to-failure in this sophisticated („open“ cross section (meso band)). Stage 3 may continue at stage 5.

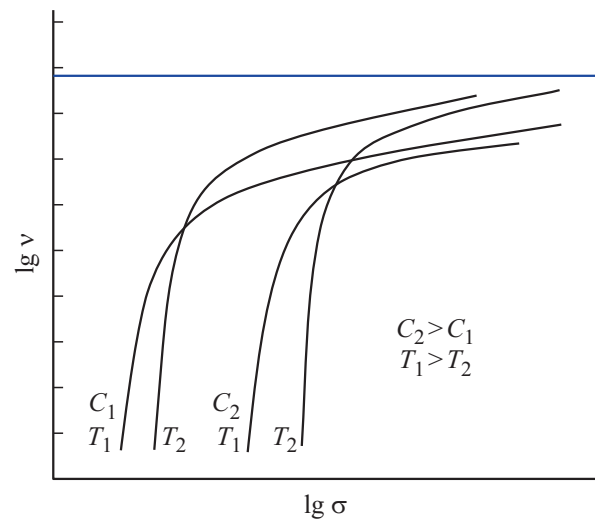


**Figure 1.** Thermally activated (low stresses) and dynamic (high stresses) dislocation rate regions  $v$  in metals depending on their strength (fault concentration  $C_2 > C_1$ ), temperature ( $T_1 > T_2$ ) and shear stress  $\sigma$  in dislocation slip plane (logarithmic scale, diagram). Horizontal line shows the sound speed level in metal.

### 3. Dislocation mobility and metal cold brittleness

Dislocation mobility defines initiation and growth of subcritical cracks and propagation of critical cracks in metals. Depending on the level of shear stress in the dislocation slip plane, dislocation mobility (slip) is characterized by thermally activated (low stresses) and dynamic (high stresses) regions [4,5,11,28,29] (Figure 1).

The thermally activated region of dislocation mobility that defines subcritical crack initiation and growth features (Figure 1):

- strong (power-law) dependence of dislocation rate  $v(\sigma)$  vs. shear stress  $\sigma$  ( $v \propto \sigma^n$ ,  $n > 1$ ).

- strong dependence of metal structure (potential crystalline pattern in the dislocation slip plane, fault concentration). Increase in metal strength (alloying, impurities, radiation-induced faults) changes dislocation movement conditions and shifts thermally activated dislocation mobility region into a higher stress region with corresponding increase in the dynamic dislocation mobility region start stress.

- dislocation rate increases with temperature rise.

In the dynamic dislocation mobility region (Figure 1) that defines critical crack propagation, the following phenomena are observed:

- linear dependence of dislocation rate vs. stress ( $v \propto \sigma$ ), which relatively weakly depends on structural (fault) state of metal,

- inverse dependence of dislocation rate vs. temperature (the lower the temperature, the higher the rate),

- asymptotic approach of dislocation rate to the sound speed.

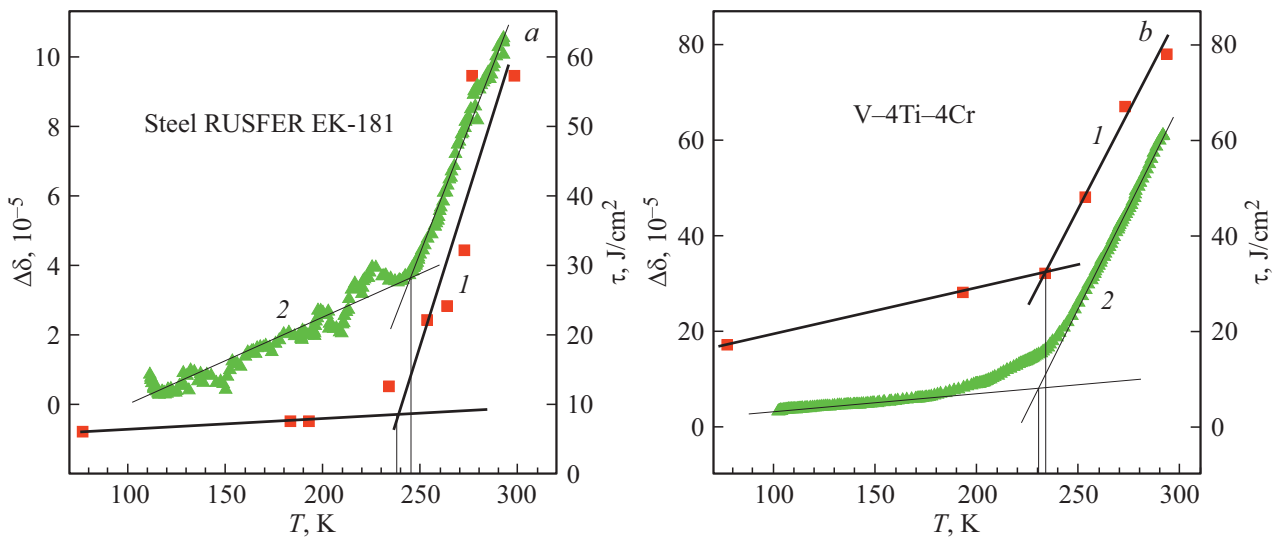


**Figure 2.** Temperature dependences: 1 — failure impact toughness energy  $\tau$ , 2 — amplitude-independent internal friction (AIIF) ( $\Delta\delta$ , UV frequency band) for ferrite-martensite steel EK-181 (RUSFER EK-181) and vanadium alloy V-4Ti-4Cr [15,19-21]. Vertical lines show physical temperatures  $T_{dbtt}$ .

Dynamic dislocation rate in shear stress  $\sigma$  is defined by  $v = (b\sigma)/B(T)$ . viscous dislocation drag coefficient  $B(T)$  is defined by interaction between dislocation and excitations (phonon-electronic) and metal crystal lattice faults depends on the metal composition and structure and generally decreases with temperature decrease [4,5,28,29]. Such aspects of  $B(T)$  define the aspects of dynamic dislocation rate in metals (Figure 1). For FCC metals, dislocation rate curves are shifted (with respect to BCC metals) towards a lower stress region depending on the stress (Figure 1) [4,5,28].

#### 4. Acoustic measurement method of cold brittleness temperature threshold (physical temperature $T_{dbtt}$ )

Non-destructive ultraviolet dynamic mechanical spectroscopy method (amplitude-independent internal friction — AIIF) allows to find temperature dependences of the viscous dislocation drag in metals [15,19–21]. AIIF level is defined in metals as a difference of its values  $\Delta\delta = \delta_2 - \delta_1$ , where  $\delta_1$  is AIIF in the initial metal sample,  $\delta_2$  is the AIIF level in the same sample after low plastic strain (introduction of „fresh“ dislocation similar to the dislocations at the crack front). Generally,  $\delta_1$  level in metals (annealed) is low and corresponds to its background value [15,19–21]. This method was used to measure [15,19–21] temperature dependences of dislocation AIIF (dislocation slip toughness) in BCC (ferrite-martensite 12% chromium steel EK-181, vanadium alloy V-4Ti-4Cr) and in FCC (austenitic chromium-nickel steel EK-164) metals at low temperatures (in cold brittleness regions of BCC metals defined by impact test method) (Figure 2 and 3).

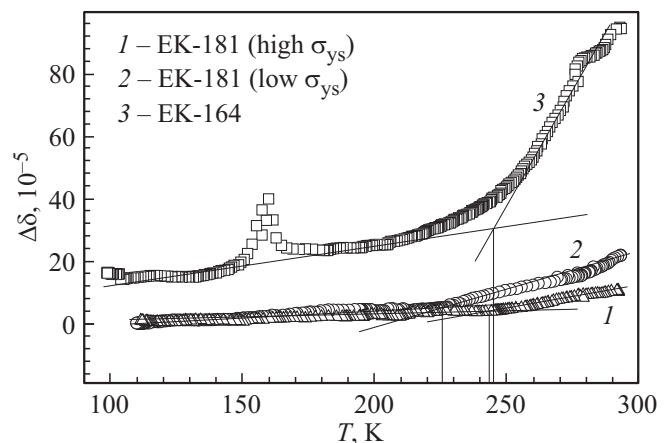


**Figure 3.** AIIF temperature dependences ( $\Delta\delta$ , UV frequency range) in ferrite-martensite steel EK-181 (two thermomechanical treatments, curves 1 and 2) and austenitic steel EK-164, curve 3 [19-21]. yield strength of steel EK-181 at stage 1 (high  $\sigma_{ys}$ ) is higher than at stage 2 (low  $\sigma_{ys}$ ). Curve 1 corresponds to curve 2 in Figure 2.

Temperature  $T_{dbtt}$  (physical cold brittleness temperature) in such experiments is defined as a temperature at which straight lines approximating adjacent low-temperature (below the knee) and subsequent high-temperature (above the knee) dependences of impact strength and internal friction intersect (Figure 2 and 3). At low temperatures (below  $T_{dbtt}$ ) in BCC metals (Figure 2 and 3), low internal dislocation friction (low viscous dislocation drag) is observed characterizing the cold brittleness state of the metals measured during the impact tests.

Typical knee of temperature dependences of impact strength and internal friction (Figure 2 and 3) is caused

by dislocation mobility depending on their impurity atmospheres. At higher temperatures (above the knees), the dislocations move together with the atmospheres, at lower temperatures (below the knees), the dislocations move without the atmospheres. When there are faults (impurities) of different grades, there may be more than one such knee with stepping on the temperature dependences of impact strength and internal friction.

Vertical lines in Figure 2 and 3 show typical cold brittleness temperatures (physical temperatures  $T_{dbtt}$ ). Close values of these typical temperatures for impact strength and internal friction are observed, which allows to derive  $T_{dbtt}$  from non-destructive acoustic tests.  $T_{dbtt}$  measured using this method will be a little lower than its value („half-brittleness“ temperature) derived during the impact tests of the metal as a temperature half-range between the upper and lower temperature beds of impact strength (or as 50% ratio of viscous and brittle failure fractions on the failure surface) [6,8,10,14,16].

The experiments show some differences in temperature dependences of metal impact strengths measured for Charpy type samples with different geometry (different stress states) and presence (absence) of cracks in the notch tips. For samples without a crack in the notch tips, impact energy will include an additional crack initiation effort. Such differences in the sample geometry will define some uncertainty in  $T_{dbtt}$  measurement („half-brittleness“ temperature). Acoustic experiments determine dynamic dislocation mobility condition in plastic zones of critical fractures and temperature region of their dynamic propagation (physical cold-brittleness temperature threshold  $T_{dbtt}$ ).

Modifications of structural phase and fault states and low-temperature strength of cold-brittle metals (alloying, phase particles, impurities, radiation-induced faults, thermomechanical treatments, irradiation) change the start stresses for dislocation generation (placement) and dynamic dislocation mobility in plastic zones of cracks and, thus, change the impact strength values and cold brittleness temperature region of metals (change  $T_{dbtt}$ ) [6,8,10,14–21,31–33]. Experiments generally show correlation between  $T_{dbtt}$  and low-temperature strength properties (yield strengths) in cold-brittle metals. Figure 3 (curves 1 and 2) illustrates such conclusions by means of ferrite-martensite steel EK-181 with different yield strengths (different thermomechanical treatment conditions) and different  $T_{dbtt}$  measured by means of the impact tests and internal friction tests [15,19–21,32,33]. Similar changes in cold brittleness temperature regions (changes in  $T_{dbtt}$ ) are also observed in V–4Ti–4Cr [19–21], vanadium alloys that have some differences in strength properties (low-temperature yield strengths) due to some differences in compositions (different concentrations of C, O, N).

In austenitic steels (as shown by means of steel EK-164, Figure 3), a typical knee is observed on the temperature dependence of internal friction. Temperatures of such knees are close for BCC and FCC metals (Figure 2 and 3), but low temperatures (viscous dislocation drag) that follow after the knees are higher in FCC metals than that in BCC metals.

High viscous dislocation drag at low temperatures defines (and at low Peierls barriers) the absence of dislocation mobility region in FCC metals and, thus, the absence of cold brittleness condition (see Section 5.2).

## 5. BCC, FCC and HCP metal dislocations and cold brittleness

Cold brittleness condition and dislocation mechanisms of brittle failure in such state of metals depend on their geometry and stress states induced by external stress. Stress in the tip of a growing crack (external stress riser) gradually achieves (with growth) some typical critical values (see Section 2.2) that define the start of strain processes in the metal (dislocation slip threshold, mechanical twinning, shear, separation). Stress relaxation in the tip of the growing subcritical crack due to strain processes of various nature (dislocation slip, mechanical twinning, etc. [4,5,27,35]) terminates its further growth. In this case, no cold brittleness state of metal is formed.

Modifications of alloy and steel compositions (alloying, impurities, irradiation) change structural phase states and properties of alloys and steels (dislocation slip systems and mobility, mechanical twinning, stacking fault energies, height of Peierls barriers, phonon-electronic excitations, viscous dislocation drag). Such modifications can change relationships between critical stresses for crack initiation and growth (see Section 2) and suppress cold brittleness initiation conditions ( $T_{dbtt}$ ) and brittle failure mechanisms in alloys and steels compared with matrix metals.

### 5.1. BCC metal cold brittleness

High-melting BCC metals are characterized by high Peierls barriers ( $10^{-3}$ – $10^{-2}G$ ) [4,5,27,30,34]. System  $\{110\}\langle 111 \rangle$  ( $\{112\}\langle 111 \rangle$  in Ta) is the main dislocation slip system in BCC metals at low temperatures [4,5,27]. Plane  $\{110\}$  is the most closely packed plane, and plane  $\{112\}$  is the main stacking fault plane [4,5]. Burgers vector direction  $\langle 111 \rangle$  is the odd center line and such types of dislocations have strong elastic interaction with point substitutional and interstitial faults [4,5,23].

High stacking fault energies in high-melting BCC metals define the absence of relaxation processes (mechanical twinning) in the tip of growing subcritical crack in them. The subcritical crack achieves the critical crack size (metal separation) in its tip (see Section 2.2). High start stresses (high Peierls barriers, faults), low viscous dislocation drag levels (Section 4, „dry friction“ condition) form dynamic dislocation mobility in the plastic zone of the critical crack at low temperatures (below  $T_{dbtt}$ ) and define fast dynamic propagation of the critical crack (metal separation) and cold brittleness initiation in high-melting BCC metals (except Ta).

Tantalum metal is the only (known) high-melting BCC metal that does not have cold brittleness [16,34,36,37]. Strain-stress properties of Ta (elastic moduli, strength,

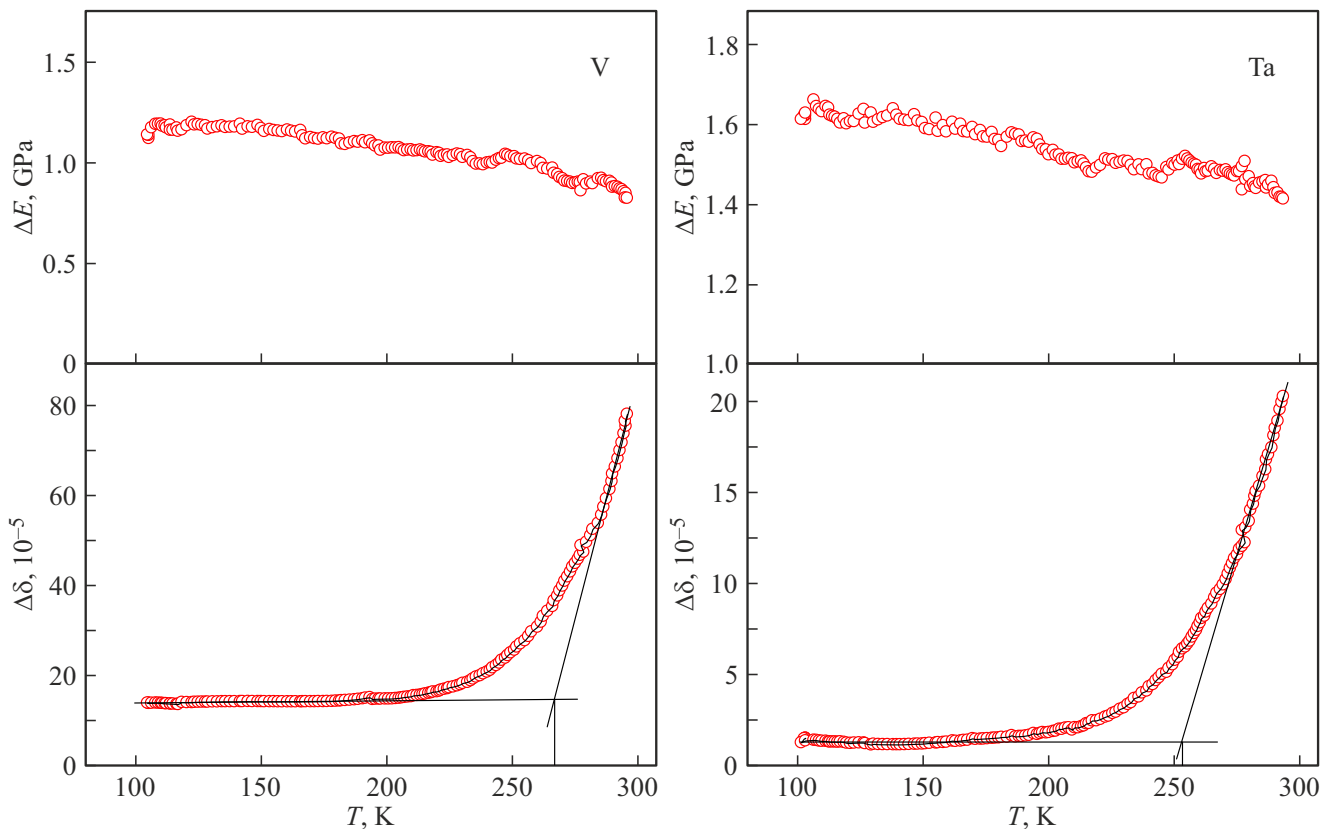


**Figure 4.** Temperature changes of Young's modulus  $\Delta E$  and AIIF  $\Delta\delta$  of vanadium samples (left figure) and tantalum samples (right figure) (B.K. Kardashev).

ductility) are typical for high-melting BCC metals. Ta features high low-temperature yield strength that increases considerably with temperature decrease [16,34], and high Peierls barrier [30]. Unlike other high-melting BCC metals, Ta has different low-temperature dislocation slip system ( $\{112\}\langle 111\rangle$ ) and high low-temperature elastic anisotropy  $A = 1.56$  ( $A = 2c_{44}/(c_{11}-c_{12})$ ,  $c_{44}$ ,  $c_{11}$ ,  $c_{12}$  — elastic constants, for other high-melting BCC metals  $A \leq 1$ ) [4,5]. Plane  $\{112\}$  in Ta is the stacking fault initiation plane. Stacking fault energy in Ta is the lowest compared with those in other high-melting BCC metals [4,5,16,27]. Stress relaxation (mechanical twinning) in the tip of the growing crack in Ta starts when the crack has its subcritical size (critical for mechanical twinning start). The growing subcritical crack in Ta does not achieve its critical size that defines Ta cold brittleness (subcritical crack stops). The absence of cold brittleness in Ta shows that the viscous drag level and dynamic dislocation mobility does not play the leading role in cold brittleness initiation (Figure 4). But the AIIF level in Ta is lower (lower viscous dislocation drag) than in vanadium (Figure 4).

Lower viscous dislocation drag in Ta at low temperatures will facilitate stress relaxation (mechanical twinning) in the tip of the subcritical crack. Ta features specific low-temperature ductility mechanisms at the crack front (mechanical twinning, polar twinning mechanism [4,5]) that are defined in Ta by high elastic anisotropy, low stacking

fault energy (low critical stress for mechanical twinning, Section 2.2) and low viscous dislocation slip resistance.

## 5.2. Absence of cold brittleness in FCC metals

FCC metals feature (compared with BCC metals) lower low-temperature yield strengths that slightly increase with temperature decrease, and lower Peierls barriers ( $\sim 10^{-5}G$ ) [4,5,27–30]. System  $\{111\}\langle 110\rangle$  is the main dislocation slip system in FCC metals [4,5]. This system features even center lines for Burgers vector  $\langle 110\rangle$ . This type of dislocations has weak elastic interaction with faults [4,5,23]. FCC metals are virtually free of start stresses for dislocation slip („dry friction“ condition for dynamic dislocation rate is not implemented). Also, the most closely-packed plane  $\{111\}$  in FCC metals is the mechanical twinning plane [4,5]. In such conditions, together with high dynamic low-temperature viscous drag of slipping dislocations (Section 4), low Peierls barriers, weak elastic interaction between dislocations and faults, and stress relaxation (mechanical twinning) at the subcritical crack fronts, no cold brittleness is initiated in FCC metals.

## 5.3. HCP metal cold brittleness

In HCP metals, dislocation slip systems both with even Burgers vector center line ( $(11-20)$  type) and odd

Burgers vector center line ( $\langle 11-23 \rangle$  type) directions are implemented (possible) [4,5,23]. Implementation of dislocation slip systems in HCP metals (alloys) is defined by crystal lattices ( $c/a$  ratio), compositions and microstructure (potential dislocation slip plane pattern). Basal, prismatic and pyramidal lattice planes may be the dislocation slip and mechanical twinning planes in HCP metals. The following shall be expected:

- HCP metals with  $\langle 11-20 \rangle$  type Burgers vectors (even center lines, prismatic and basal dislocation slip planes) will have cold brittleness properties similar to that of FCC metals (no cold brittleness).
- HCP metals with  $\langle 11-23 \rangle$  type Burgers vectors (odd center lines, pyramidal dislocation slip planes) will have cold brittleness properties similar to that of BCC metals (cold brittleness is possible).

## 6. Influence of reactor irradiation on metal cold brittleness

Structure states, elemental compositions and properties of metals „before — during — after“ reactor (neutron, gamma) irradiation vary considerably. cold brittleness of metals „before“ irradiation is addressed above (see 2–5).

### 6.1. Cold brittleness of metals after irradiation

In conditions „before–after“ irradiation, a thermodynamically-(quasi)equilibrium state is formed (with temperature as the governing parameter). After the low-temperature irradiation of metals, thermodynamically-nonequilibrium state of their structure, low-temperature strength and  $T_{dbtt}$  increase (low-temperature irradiation embrittlement - LTIB). Typical features of cold brittleness temperature properties of metals (cold-brittle „before“ irradiation) are observed „after“ the low-temperature irradiation [31–33,38–40]:

- expansion (shift) of the cold brittleness temperature region of metals ( $T_{dbtt}$  increase, LTIB) with irradiation dose increase,
- decrease of the upper impact strength temperature bed level,
- change (reduction) in slopes of temperature dependences of impact energies,
- annealing of irradiated metals (products) brings the cold brittleness temperature region and properties almost in their initial state.

Changes in cold brittleness of metals „after“ irradiation depend on the irradiation time and temperature and holding time (nuclear cooling, residual radioactivity) after irradiation and are characterized by the above cold brittleness initiation conditions and brittle failure mechanisms in metals. Such cold brittleness changes occur due to modifications of their elemental compositions (nuclear transmutations), structure (radiation-induced faults, ordering), residual radioactivity and stress-strain properties (elasticity, strength, etc.).

Irradiation-induced („post“-irradiation) changes in temperature and dose dependences of impact strength (LTIB)

may result in the loss of ductility and brittle failure of metals not only due to shear ( $T_{dbtt}$  increase), but also due to reduction (temperature slope increase) of the impact strength level the irradiated metals (products).

The low-temperature irradiation embrittlement phenomenon (LTIB) in metals (results after the irradiation test) necessitates (on an unjustified assumption of maintaining this phenomenon „during“ irradiation) increasing the lower reactor operating temperature (fast, nuclear fusion), restricting irradiation loads on metals (restricting reactor fuel cycle times) and intermediate annealing of the irradiated metals (products). However, such conclusion requires clarification of conditions and identification of cold brittleness (non)occurrence mechanisms in metals (cold brittle „before–after“ irradiation) „during“ irradiation operations.

### 6.2. Cold brittleness of metals „during“ reactor irradiation

States and properties of metals „during“ reactor (neutron, gamma) irradiation differ considerably from the states „before–after“ irradiation [17,18,39–45]. „During“ irradiation, the state of metals becomes significantly more nonequilibrium (matter and energy inflow from the environment) with enhancement of openness–nonequilibrium state and initiation of dynamic steady state of the structure supported by radiation exposure. Irradiation intensity is the governing parameter of such dynamic irradiation state of metal. Such nonequilibrium structures and properties of metals „during“ irradiation may be studied with the involvement of their behavior.

„During“ irradiation, various dynamic processes (heat and mass flows, temperature gradients, „initiation–death“ of irradiation-induced faults, radiation „bounce“, ionization) occur and induce additional volume stress constants and variables (acoustic noise) [17,18,39–45]. In such irradiation conditions, atom energy properties (interatomic interaction energies, radiation displacement energy thresholds, diffusion properties) and stress-strain properties (reduction of moduli of elasticity and strength, occurrence of irradiation-induced creep without thermal creep) are changed in metals [17,18,39–48]. Dynamic irradiation conditions („radiation bounce“) enhance the dislocation mobility (reduce start stresses) and stress relaxation at the subcritical crack fronts. In such conditions, no critical cracks are initiated (no „dry“ friction condition is initiated for dynamic dislocation slip at the crack fronts). In metals (cold brittle „before–after“ irradiation), no cold brittleness is initiated „during“ low-temperature irradiation [17,18].

Gamma-component of irradiation has a considerable influence on structure state and stress-strain properties of metals [41,49–52]. Gamma fluxes in nuclear and nuclear fusion reactors are formed by ( $n-\gamma$ ) type nuclear reactions on the nuclear fuel and structural materials (steels, alloys) elements. Intensities of gamma fluxes significantly differ in fission reactors (additional flux from nuclear fuel) and fusion reactors. Gamma irradiation has a negligent

influence on the irradiation-induced fault rate of metals (irradiation-induced displacements per atom) compared with neutron displacements per atom [51]. Influence of gamma irradiation appears through atom ionization, change in electronic density and interatomic interactions that change energy properties of atoms (mobility, displacement energy thresholds) in metals and their stress-strain properties (loss of strength, stress relaxation).

Differences in structural states (thermodynamic and dynamic equilibrium states) and metal properties „before — during — after“ irradiations (neutron, gamma) define the limited results obtained in conditions „before—after“ metal irradiation for identification of their structures and properties „during“ irradiations (during reactor operation). Investigations of structures and stress-strain properties of irradiated metals („after“ irradiation), including cold brittleness, in order to determine the structures and stress-strain properties „during“ irradiations are insufficiently representative and informative for the development of structural materials (products) for next generation nuclear and nuclear fusion reactors. Differences in irradiation conditions (neutron and gamma spectra) in fission and fusion reactors also define the differences in structure formation, elemental compositions and properties in („during — after“) irradiation conditions in fission and fusion reactors. Such differences define limited use of materials tests in fission (fast, etc.) reactors for the purpose of nuclear fusion reactors.

## 7. Conclusion

1. Conditions and dislocation mechanisms of cold brittleness initiation (ductile-brittle transition temperature  $T_{dbtt}$  generation, brittle failure at stresses lower than yield strengths) in metals (alloys, steels) are determined in conditions „before — during — after“ irradiations (neutron, gamma). cold brittleness of metals is a multistage structural process (in space and time) whose all stages are dislocational and are controlled by initiation of subcritical and critical cracks and stress at crack fronts. High start stresses (high Peierls barrier, faults) for dislocation slip, low viscous dislocation drag and high dislocation rate in plastic zones of critical cracks form cold brittleness conditions in metals.

Cold brittleness stages in metals are controlled by thermally activated (initiation and growth of subcritical cracks) and dynamic (dynamic propagation of critical cracks) dislocation mobilities. Dislocational mechanisms of metal (alloy, steel) cold brittleness are defined by metal crystal lattices (BCC, FCC, HCP), elemental compositions, microstructure states (thermodynamic and dynamic equilibrium levels), dislocation slip systems and mobilities, stacking and surface fault energies, and stress-strain properties (elasticity, strength, ductility) at certain temperature and stress states.

2. Stress relaxation in tips of growing subcritical cracks stops their growth (no cold brittleness is initiated). stacking fault energy defines the stress relaxation (mechanical twinning, etc) threshold level in the tips of cracks. cold

brittleness of metals reduces with a decrease in stacking fault energy (decrease in critical stress for mechanical twinning). Metals with closely-packed lattices (FCC, HCP) are less cold-brittle due to low stacking fault energies. Metal alloying reduces the stacking fault energy and suppresses cold brittleness of alloys and steels on the basis of such (matrix) metals.

The absence of cold brittleness in Ta is caused by its specific nature of low-temperature ductility (low stress for mechanical twinning) due to low stacking fault energy.

3. Structure state (equilibrium levels) and stress-strain properties of metals in conditions „before — during — after“ reactor irradiation (neutron, gamma) differ considerably. Gamma-component of reactor irradiation has a considerable influence on the structure state and properties of metals. In irradiated metals (cold brittle „before“ irradiation), cold brittleness temperature region is expanded ( $T_{dbtt}$  is increased). „During“ low-temperature irradiation of metals (cold brittle „before—after“ irradiation), no cold brittleness condition is formed (no cold brittleness of metals „during“ irradiation).

4. Differences in structure states and metal properties „before — during — after“ reactor irradiations (neutron, gamma) define the limited scope of application of the results (experimental, theoretic, simulation) obtained in conditions „before—after“ irradiation for identification of metal structures and properties „during“ irradiations.

## Acknowledgments

The author would like to express gratitude to B.K. Kardashev (Ioffe FTI of RAS) for fruitful discussions of metal cold brittleness issues and for acoustic measurements of elastic moduli and internal friction in metals.

## Conflict of interest

The author declares that he has no conflict of interest.

## References

- [1] A.A. Griffith. *Phil. Trans. Roy. Soc. Ser. A* **221**, 582, 163 (1920).
- [2] E.V. Stepanov. *Osnovy prakticheskoy prochnosti kristallov*. Nauka, M. (1974). 132 p. (in Russian).
- [3] B.A. Drozdovsky, Ya.B. Fridman. *Vliyanie treshchin na mekhanicheskie svoistva konstruktsionnykh staley*. Metallurgiya, M., (1960). 260 p. (in Russian).
- [4] J. Friedel. *Dislocations*. Pergamon Press, Oxford (1964). 580 p.
- [5] J.P. Hirth, J. Lothe. *Theory of dislocations*. McGraw-Hill Book Company (1970). 599 p.
- [6] B.M. Finkel. *Phisika razrusheniya*. Metallurgiya, M., (1970). 376 p. (in Russian).
- [7] *Atomistics of Fracture* / Eds R.M. Latanision, J.R. Pickens. Plenum Press, N.Y. (1983). 1074 p.
- [8] A.Ya. Krasovsky. *Khrupkost metallov pri nizkikh temperaturakh*. Nauk. dumka, Kiev, 1980). 338 p. (in Russian).
- [9] V.L. Indenbom. *JETP Lett.* **12**, 11, 369 (1970).

- [10] V.I. Vladimirov. Fizicheskaya priroda razrusheniya metallov. Metallurgiya, M., (1984). 280 s. (in Russian).
- [11] Elastic strain fields and dislocation mobility / Eds V.L. Indenbom, J. Lothe. Elsevier Sci., N.H. (1992). 778 p.
- [12] V.E. Panin, V.E. Egorushkin. Phys. Mesomech. J. **11**, 3–4, 105 (2008).
- [13] D.S. Kryzhevich, A.V. Korchuganov, K.P. Zolnikov. Res. Phys. **33**, 7285, 105163 (2022).
- [14] V.M. Chernov, G.N. Ermolaev, M.V. Leont'eva-Smirnova. Tech. Phys. **55**, 7, 985 (2010).
- [15] B.K. Kardashev, V.M. Chernov. Phys. Solid State **50**, 5, 854 (2008).
- [16] M.A. Shtremel. Razrusheniye. Kn. 1: Razrushenie materiala. Izd. dom MISiS, M. (2014). 670 p. Kn. 2: Razrushenie struktur. Izd. dom MISiS, M. (2015). 976 p. (in Russian).
- [17] V.M. Chernov, K.A. Moroz. Atomic Energy **122**, 2, 93 (2017).
- [18] V.M. Chernov. Perspektiv. materialy **23**, 2018 (2004). (in Russian).
- [19] B.K. Kardashev. Crystallogr. **54**, 6, 1021 (2009).
- [20] V.M. Chernov, B.K. Kardashev, K.A. Moroz. Nucl. Mater. Energy **9**, 496 (2016).
- [21] V.M. Chernov, B.K. Kardashev, K.A. Moroz. Tech. Phys. **61**, 7, 1015 (2016).
- [22] V.L. Indenbom. The microscopic theory of cracks. In: [11]. P. 253–268.
- [23] V.L. Indenbom, V.M. Chernov. Thermally activated glide of a dislocation in a point defect field. In: [11]. P. 517–570.
- [24] V.L. Indenbom, V.M. Chernov. FTT **21**, 5, 1311 (1979). (in Russian).
- [25] M.P. Zhetbaeva, V.L. Indenbom, V.V. Kirsanov, V.M. Chernov. Pisma v ZhTF, **1157** (1979), 19 (2020). (in Russian).
- [26] V.M. Chernov, D.A. Kamaev. Nelineynaya dinamika dislokatsiy v polyakh vnutrennikh napryazheniy pri sovместnom deistvii postoyannykh i peremennykh nagruzok. Preprint FEI-2497. Obninsk (1996). 34 p. (in Russian).
- [27] Metallovedenie / Pod red. V.S. Zolotarevskogo. Izd. dom MISiS, M. (2014). T. 1. 496 p. (in Russian).
- [28] E.M. Nadgorny. Dislocation Dynamics and Mechanical Properties of Crystals. Pergamon Press, Oxford (1988). 530 p.
- [29] V.I. Alshits. The phonon-dislocation interaction and its role in dislocation dragging and thermal resistivity. In: [11]. P. 625–698.
- [30] P. Guyot, J.E. Dorn. V Sb.: P. Guyot, J.E. Dorn. A.N. Orlov (red.). Aktual'nye voprosy teorii dislokatsiy / Mir, M. (1988), C. 270–310. (in Russian).
- [31] A.G. Ioltukhovskiy, M.V. Leonteva-Smirnova, M.I. Solonin, V.M. Chernov, V.N. Golovanov, V.K. Shamardin, T.M. Bulanov, A.V. Povstyanko, A.E. Fedoseev. J. Nucl. Mater. **307–311**, Part 1, 532 (2002).
- [32] M.V. Leont'eva-Smirnova, A.N. Agafonov, G.N. Ermolaev, A.G. Ioltukhovskiy, E.M. Mozhanov, L.I. Reviznikov, V.V. Tsvelev, V.M. Tchernov, T.M. Bulanov, V.N. Golovanov, Z.O. Ostrovskiy, V.K. Shamardin, A.I. Blokhin, M.B. Ivanov, E.N. Kozlov, Yu.R. Kolobov, B.K. Kardashev. Perspektiv. materialy **6**, 40 (2006). (in Russian).
- [33] V.M. Chernov, M.V. Leonteva-Smirnova, M.M. Potapenko, N.I. Budylkin, Yu.N. Devyatko, A.G. Ioltoukhovskiy, E.G. Mironova, A.K. Shikov, A.B. Sivak, G.N. Yermolaev, A.N. Kalashnikov, B.V. Kuteev, A.I. Blokhin, N.I. Loginov, V.A. Romanov, V.A. Belyakov, I.R. Kirillov, T.M. Bulanov, V.N. Golovanov, V.K. Shamardin, Yu.S. Strebkov, A.N. Tyumentsev, B.K. Kardashev, O.V. Mishin, B.A. Vasiliev. Nucl. Fusion **47**, 8, 839 (2007).
- [34] J.H. Bechtold. Acta Metallurgica **3**, 3, 249 (1955).
- [35] A.N. Tyumentsev, A.D. Korotaev, I.A. Ditenberg, Yu.P. Pinzhin, V.M. Chernov. Zakonomernosty plasticheskoy deformatsii v vysokoprochnykh i nanokristallicheskiy metallicheskiy materialakh. Nauka, Novosibirsk (2018). 256 p. (in Russian).
- [36] I.I. Kornilov, V.V. Glazova. Vzaimodeystvie tugoplavkikh metallov perehodnykh grupp s kislorodom. Nauka, M. (1967), 256 p. (in Russian).
- [37] A.P. Gelyaev. Korroziionostoikie splavy tugoplavkikh metallov. Nauka, M. (1982), 120 p. (in Russian).
- [38] R.L. Klueh, D.R. Harris. High-chromium Ferritic and Martensitic Steels for Nuclear Applications. ASTM Int. (2001).
- [39] L.I. Ivanov, Yu.M. Platov. Ragiatsionnaya fizika metallov i eyo ptolozheniya. Interkontakt Nauka., M. (2002). 300 p. (in Russian).
- [40] V.V. Voyevodin, I.M. Neklyudov. Evolyutsiya strukturno-fazovogo sostoyaniya i radiatsionnaya stoikost konstruksionnykh materialov. Nauk. dumka, Kiev, 2006). 376 p. (in Russian).
- [41] V.P. Krivobokov, S.N. Yanin. Atomic Energy **131**, 1, 17 (2021).
- [42] Physics of radiation effects in crystals / Eds R.A. Johnson, A.N. Orlov. Elsevier Sci., N.H. (1986). 723 p.
- [43] V.V. Slezov, P.A. Bereznayak. In: [42]. P. 575–620.
- [44] R. Bullough, M.H. Wood. In: [42]. P. 189–224.
- [45] H. Wiedersich. In: [42]. P. 225–280.
- [46] V.M. Chernov, O.V. Kamaeva. Mater. Sci. Eng. A **370**, 1–2, 246 (2004).
- [47] B.K. Kardashev, V.M. Chernov, O.A. Plaksin, V.A. Stepanov, L.P. Zavialski. J. Alloys. Compounds **310**, 1–2, 102 (2000).
- [48] V.M. Chernov. Phys. Solid State **46**, 8, 1449 (2004).
- [49] V.A. Nikolaenko, V.I. Karpukhin. J. Nucl. Mater. **233–237**, Part 2, 1067 (1996).
- [50] V.A. Nikolaenko, V.I. Karpukhin, E.A. Krasikov, V.N. Kuznetsov. J. Nucl. Mater. **271–272**, 120 (1999).
- [51] F.A. Garner, L.R. Greenwood, P. Roy. In: Effects of radiation on materials: 18th Int. Symp. ASTM STP 1325, ASTM (1999). P. 52–74.
- [52] S.N. Yanin. IOP Conf. Ser.: Mater. Sci. Eng. **81**, 1, 012061 (2015). DOI: 10.1088/1757-899X/81/1/012061

Translated by E.Ilyinskaya